Article

Synthesis and Structure-Activity Relationships of Resorcinol Derivatives as Highly Potent Tyrosinase Inhibitors

You Zhou [1], Qihang Li[2], Ronggeng Fu [3], Hongyu Yang [2], Jun Mo [2], Yao Chen [4] and Qingyou Xia [5,*]

[1] College of Biotechnology, Southwest University, Chongqing 400715, China; zhouy701005@swu.edu.cn
[2] School of Pharmacy, China Pharmaceutical University, Nanjing 210009, China; liqihangcpu@163.com(L.Q.); 331378880@qq.com (H.Y.); 1557752492@qq.com (J.M.)
[3] School of Pharmacy, Hunan University of Chinese Medicine, Changsha 410208, China; furonggeng@hnucm.edu.cn
[4] School of Pharmacy, Nanjing University of Chinese Medicine, Nanjing 210023, China; 394702066@qq.com
[5] State Key Laboratory of Silkworm Genome Biology, Southwest University, Chongqing 400715, China; xiaqy@swu.edu.cn
* Correspondence: xiaqy@swu.edu.cn; Tel.: +86-139-9636-8108

Abstract: Compounds with tyrosinase inhibitory efficacy could be effective as depigmenting agents. Although a large number of natural and synthetic tyrosinase inhibitors have been reported, few of them are used as skin-whitening agents due to poor activity and safety concerns. 3-(2,4-Dihydroxyphenyl)propionic acid (DPPA), a naturally occurring compound isolated from *Ficus carica*, was previously discovered as a moderate tyrosinase inhibitor. In this study, the structure-activity relationship study of DPPA was conducted. Compound **3g**, with the 2,4-resorcinol subunit and terminal hydrophobic di-butylamino group, was identified with low nanomolar enzymatic IC_{50} value. Additionally, compound **3g** could effectively reduce melanin levels in B16-F10 melanoma cells treated with α-melanocyte-stimulating hormone (α-MSH) without affecting cell viability and proliferation. All these results indicated that compound **3g** could be considered as a promising candidate for the treatment of diseases associated with hyperpigmentation.

Keywords: hyperpigmentation; tyrosinase inhibitors; 3-(2,4-dihydroxyphenyl)propionic acid; structure-activity relationship study; B16-F10 cellular melanogenesis inhibition

1. Introduction

Tyrosinase [EC 1.14.18.1] is a multifunctional copper-containing enzyme widely distributed in nature and is a key enzyme in the biosynthesis of melanin pigments. It is well-known that tyrosinase can catalyze the first two steps in the conversion of tyrosine to melanin: hydroxylation of tyrosine to L-DOPA and oxidation of L-DOPA to dopaquinone [1]. Previous investigations have shown that this enzyme was responsible not only for the browning of some fruits and vegetables, decreasing the commercial value of the produce, but also for the formation of some dermatological problems, such as melisma, postinflammatory melanoderma, age spots and freckles[2]. Moreover, tyrosinase is important for the insect moulting process[3] and adhesion in marine organisms[4]. Furthermore, melanin pigments are found in the mammalian brain, and tyrosinase activity is linked to neurodegeneration associated with Parkinson's[5], Alzheimer's, and Huntington's diseases. Thus, seeking potent tyrosinase inhibitors is a major concern in agricultural, pharmaceutical and cosmetic fields. The well-known tyrosinase inhibitors include hydroquinone, arbutin and kojic acid. [6]Unfortunately, most reported compounds are generally limited in practical application with regard to their poor potency and high cytotoxicity[7]. Thus, it is necessary to search for and develop

novel tyrosinase inhibitors with excellent potency and a low toxicity to resolve issues related to the tyrosinase activity.

So far, crystal structures from different species such as plant (e.g., *Juglans regia*), mushroom (e.g., *Agaricus bisporus*), and bacteria (e.g., *Bacillus megaterium*) were reported. While preliminary crystallographic studies on human tyrosinase have been reported very recently, no structures are available to date at atomic resolution. In general, the structure of tyrosinase can be classified into three domains, namely, the central, the N-terminal, and the C-terminal domains[8]. Among tyrosinases from different species, the central domain is the most conserved domain, which comprises two close copper centers (CuA and CuB) coordinated by six histidine residues[9]. To obtain new potent tyrosinase inhibitors (> To study/investigate the mode of inhibition (or mode of action) of tyrosinase inhibitors in an atomic level, we used mushroom tyrosinase in our study since its X-ray crystal structure and *in vitro* tyrosinase assay were available). In addition, mouse B16-F10 melanoma cell line, a tyrosinase-expressing cell line, was employed to investigate the tyrosinase activity across species in the presence of our compound by performing cytotoxicity and melanin biosynthesis assays. As we know, mushroom tyrosinase and murine tyrosinase share 58% identity within 6 Å of the two copper centers.

DPPA, is a naturally occurring tyrosinase inhibitor isolated from *Ficus carica*, with reported IC_{50} of 3.2 μM[10]. Previous efforts have proved that chemical modification of carboxyl group of DPPA could augment its tyrosinase inhibitory activity[11]. Compared to other natural and synthetic substances, it shows superiority in designing tyrosinase inhibitors for following reasons: (1) the resorcinol scaffold can induce tyrosinase inactivation by the Quintox inactivation mechanism in which a portion of the resorcinol substrate is subjected to monooxygenase action leading to irreversible elimination of Cu^0 from the active site; (2) the short synthetic route of DPPA makes it suitable for further development. DPPA was, therefore, selected by our laboratory as an ideal starting point for the development of novel and highly potent tyrosinase inhibitors. Here, we reported the structure-activity relationship of DPPA focusing on the carboxyl group, 4-substituted resorcinol moiety, and the ethylidene linker. Anti-tyrosinase efficacy of all targeted compounds were tested and compound **3g** was identified with low nanomolar enzymatic IC_{50} values. Furthermore, compound **3g** effectively reduced melanin levels in B16-F10 melanoma cell lines treated with α-MSH without affecting cell viability and proliferation.

2. Results and Discussions

The synthesis of compounds **3a-3l** was accomplished in 2 steps (Scheme 1). The reaction between resorcinol (**1**) and acrylic acid generated compound **2**, which was involved with esterification followed by ring closure [12]. Compound **2** was then reacted with various amines in DMF to give **3a-3l** in high yield. The preparation of target compounds **5a-5f** and **7** are described in Scheme 2. Dibutylamine was reacted with various substituted phenylpropionic acids and 3-(4-chlorophenoxy)propionic acid in CH_2Cl_2 to give **5a-5f** and **7** in good yield. All target compounds were purified by column chromatography and their structures were characterized by ^1H NMR, ^{13}C NMR and HRMS.

Preprints (www.preprints.org) | NOT PEER-REVIEWED | Posted: 14 November 2018 doi:10.20944/preprints201811.0330.v1

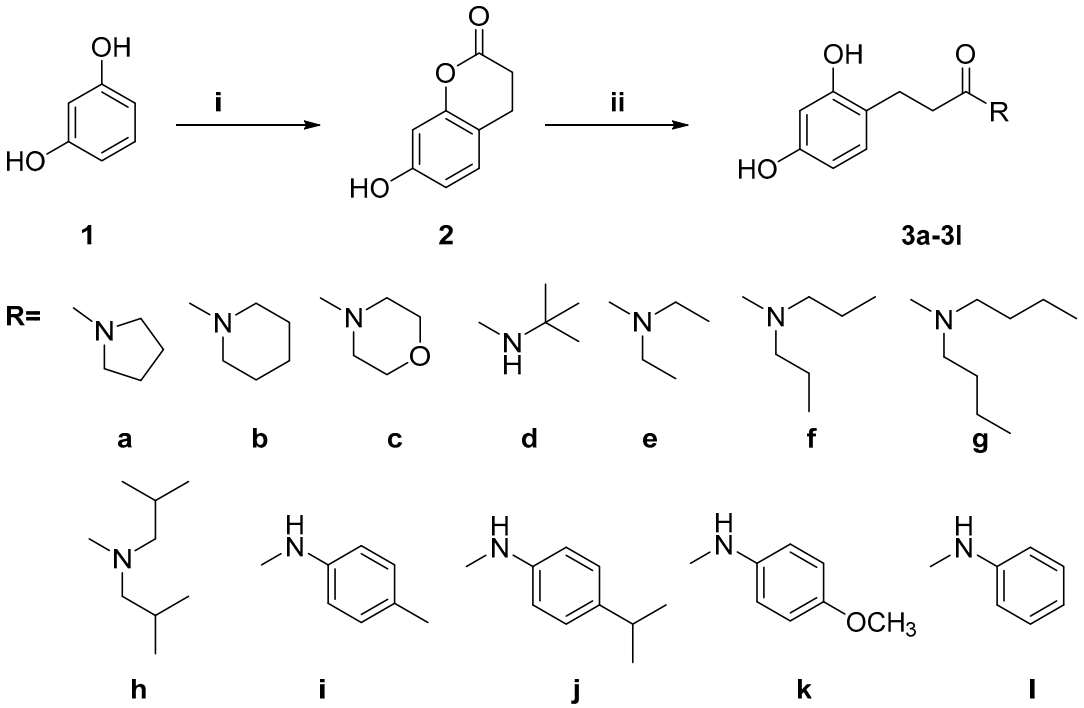

Scheme 1. Reagents and conditions: (i) CH_2=$CHCO_2H$, Amberlyst 15, toluene, reflux; (ii) amine, DMF, 100 °C.

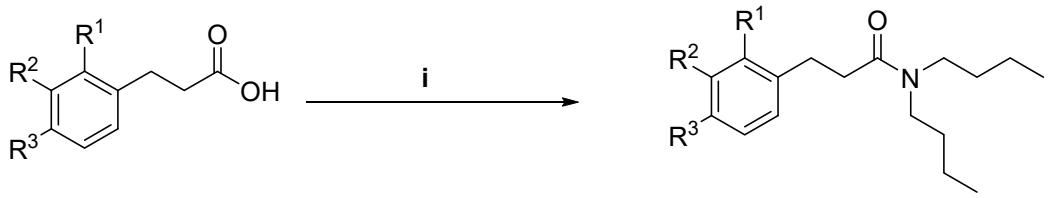

a: R^1 = OCH_3, R^2 = H, R^3 = OCH_3

b: R^1 = OH, R^2 = H, R^3 = H

c: R^1 = H, R^2 = H, R^3 = OH

d: R^1 = H, R^2 = OH, R^3 = OH

e: R^1 = Cl, R^2 = H, R^3 = H

f: R^1 = H, R^2 = H, R^3= Cl

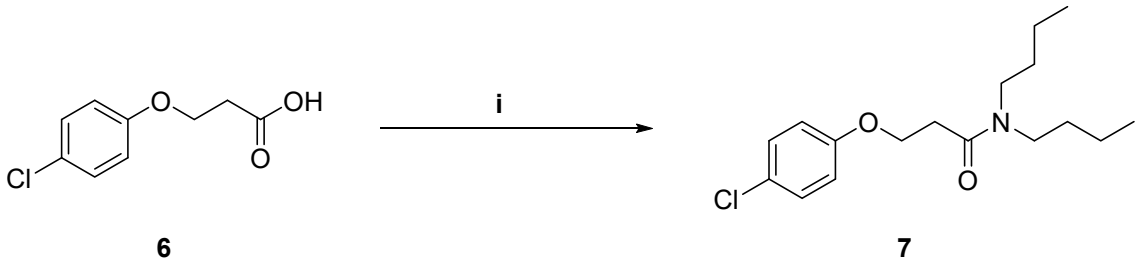

Scheme 2. Reagents and conditions: (i) CDI, CH_2Cl_2, r.t, 12h.

Anti-tyrosinase efficacy of all synthesized compounds was tested on both enzyme activities stages: L-tyrosine as substrate to L-DOPA and the oxidation of the later to o-quinone. Kojic acid, a

 doi:10.20944/preprints201811.0330.v1

well-known tyrosinase inhibitor was selected as a positive control (Table 1). Compounds 3a-3h, with the 2,4-resorcinol skeleton and different terminal amino groups indicated higher tyrosinase inhibitory activity with the first stage than that of the second stage. Compound 3g, containing a hydrophobic di-n-butylamino substituent, exhibited the best activity. As shown in Table 1, compound 3g inhibited the first stage with low nanomolar concentration (IC50 = 12.2 nM) and presented potent inhibition of the second stage (IC50 = 200.7 nM). Similarly, compounds (3a, 3f and 3h) with other terminal hydrophobic groups potently inhibited the first stage with IC50 values < 1 μM. These results, to some extent, were consistent with those found in previous study that addition of a hydrophobic moiety that contains a minor bulky group to the 2,4-resorcinol skeleton was beneficial to increase the tyrosinase inhibition potency [11]. Intriguingly, we found that the existence of terminal hydrophilic group (3b, 3d and 3e) also played an important role in biological potency, which may interact with the hydrophilic pocket around the binuclear copper ions leading to improved enzyme-inhibitor binding affinity. It is noteworthy that the introduction of morpholino group (3c) to DPPA apparently decrease its in vitro enzyme activity, suggesting that introduction of the morpholino group has a detrimental effect on the inhibition potency.

In contrast to 3a-3h, compounds 3i-3l containing different terminal phenylamino groups possessed higher tyrosinase inhibitory activity with the second stage than that of the first stage, indicating a different mode of action involved (Table 1). Compound 3i, which contains a p-methyl substituted aromatic benzene ring, inhibited the second stage with an low nanomolar concentration (IC50 = 84.8 nM) and showed potent inhibition of the first stage (IC50 = 3501.0 nM). In comparison with 3i, compounds containing unsubstituted benzene ring or other substituted benzene rings demonstrated weaker enzyme inhibitory potency with the second stage.

When the 2, 4-resorcinol subunit was replaced with other substituted benzene rings, the resulting compounds, 5a-5f, displayed very low inhibitory potency with both of the enzyme activities stages (Table 1). It suggested that the 2,4-resorcinol subunit is the key pharmacophore required for potency of the novel series of DPPA amide derivatives. In comparison with 3g, the introduction of an oxygen atom in the ethylidene linker produced the analogue (compound 7) without any inhibitory potency (Table 1).

Preprints (www.preprints.org) | NOT PEER-REVIEWED | Posted: 14 November 2018 doi:10.20944/preprints201811.0330.v1

133 **Table 1.** Inhibitory effects on mushroom tyrosinase activity of target compounds.

Compounds	L-Tyrosine (IC_{50}, nM)	L-DOPA (IC_{50}, nM)
3a	239.5	3260.0
3b	436.0	3361.0
3c	34410.0	63460.0
3d	80.3	1277.0
3e	251.4	1117.0
3f	41.6	1112.0
3g	12.2	200.7
3h	101.3	1603.0
3i	3501.0	84.8
3j	2364.0	303.4
3k	1142.0	154.8
3l	6085.0	307.3
5a	>50000	>50000
5b	>50000	>50000
5c	>50000	>50000
5d	>50000	>50000
5e	>50000	>50000
5f	>50000	>50000
7	>50000	>50000
DPPA	9031.0	8279.0
Kojic acid	9031.0	8279.0

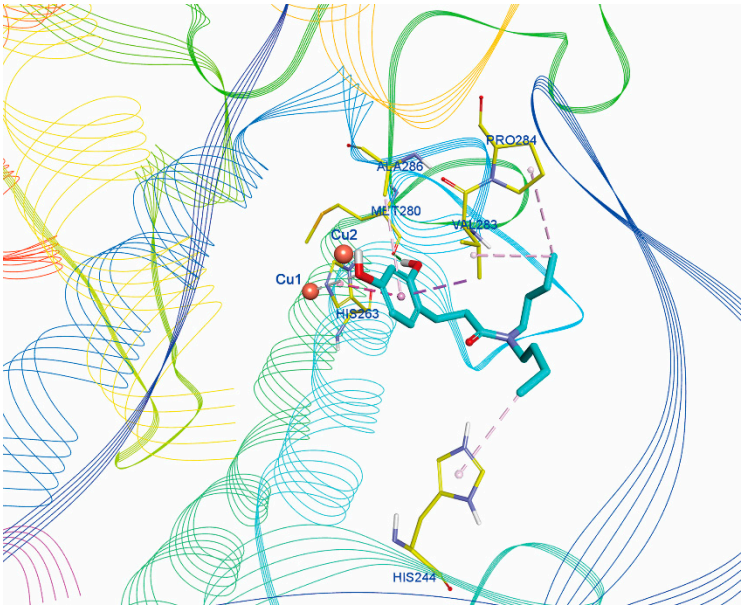

134 **Figure 1**. Binding mode prediction of compound 3g with mushroom tyrosinase (PDB ID: 2Y9X).
135 The compound is shown in cyan stick mode (carbon atoms). Key residues of mushroom tyrosinase

Preprints (www.preprints.org) | NOT PEER-REVIEWED | Posted: 14 November 2018 doi:10.20944/preprints201811.0330.v1

are depicted in yellow thin stick mode. The copper ions are represented by orange spheres. The hydrophobic contact as well as the π-π stacking are depicted in purple dot line, while H-bonds are in green dot line. Only polar hydrogen atoms are shown.

Next, the binding mode of the most active compound 3g to mushroom tyrosinase was predicted by using molecular docking method (Figure. 1). The binding mode revealed that the C2 phenolic hydroxyl group of compound 3g formed a hydrogen bond with Met280, and the C4 phenolic hydroxyl group could chelate one of the binuclear copper ions. Furthermore, hydrophobic interactions as well as π-π stacking were also found between the benzene ring of compound 3g and the side chains of His263, Val283 and Ala286. Additionally, the di-n-butylamino group at the end of 3g also could form hydrophobic interactions with His244, Val283 and Pro284. These results clearly emphasized the importance of the 2,4-resorcinol moiety and hydrophobic side chain in potent tyrosinase inhibitors.

The stability and energy profile of the docking poses of compound 3g was investigated through MD simulations and the calculations of binding free energies. In Figure 2, the RMSD values of simulation converged after about 3000 frames (60 ns), indicating that the system is stable and equilibrated. The root-mean-square deviations (RMSD) values of complex compared first conformation of MD swing at 2~3 Å indicated that the complex of 3g and tyrosinase become stable after the first short stage of variation and the docking pose is reliable.

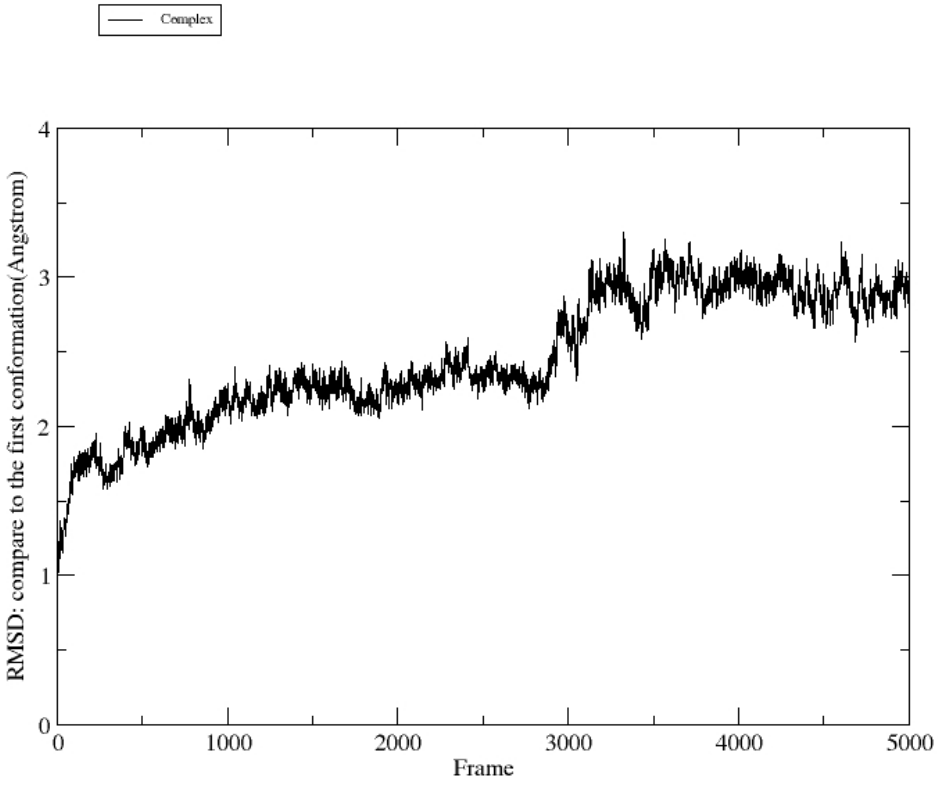

Figure 2. The RMSD values of complex 3g-tyrosinase changes with the frames of MD comparing to the first conformation of complex 3g-tyrosinase.

The MMPBSA method was used to calculated the binding free energies and gain information on the different components of interactions energy that contribute to complex 3g-tyrosinase. Detailed results are shown in Figure 3. Figure 3(a) indicates that electrostatic energy (EEL)and van der Waals energy (VDWAALS) are both vital in the binding of 3g to mushroom tyrosinase.

Preprints (www.preprints.org) | NOT PEER-REVIEWED | Posted: 14 November 2018 doi:10.20944/preprints201811.0330.v1

Non-polar solvation energy (ESURF) are also did favorable contribution to complex 3g-tyrosinase binding (-3.3965 Kcal/mol). Meanwhile, Polar solvation energy(EGB) does not favor for 3g binding. The binding free energy of compound 3g and tyrosinase is -18.8305 Kcal/mol indicates that the binding of 3g and tyrosinase is favored in terms of energy.

For identification of key residues contributing to binding affinity, we also carried out the energy decomposition analysis. As shown in Figure 3(b) and (c), the interaction energy between the residue and the ligand is negative would be considered to be hot residues, the hot residue are HIE263,MET280,VAL283 and ALA286. These hot residues and energy decomposition analysis provides a theoretical basis for further lead optimization and discussions.

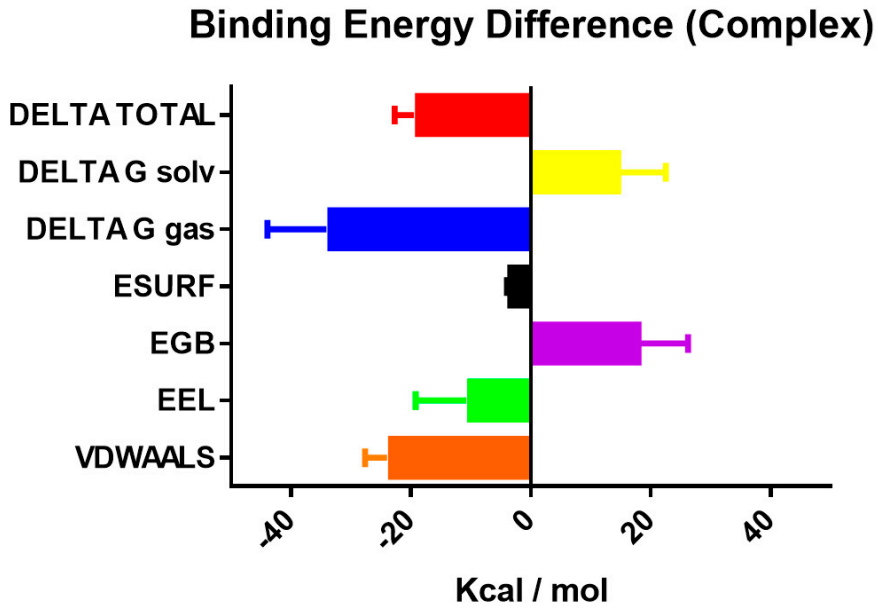

(a)

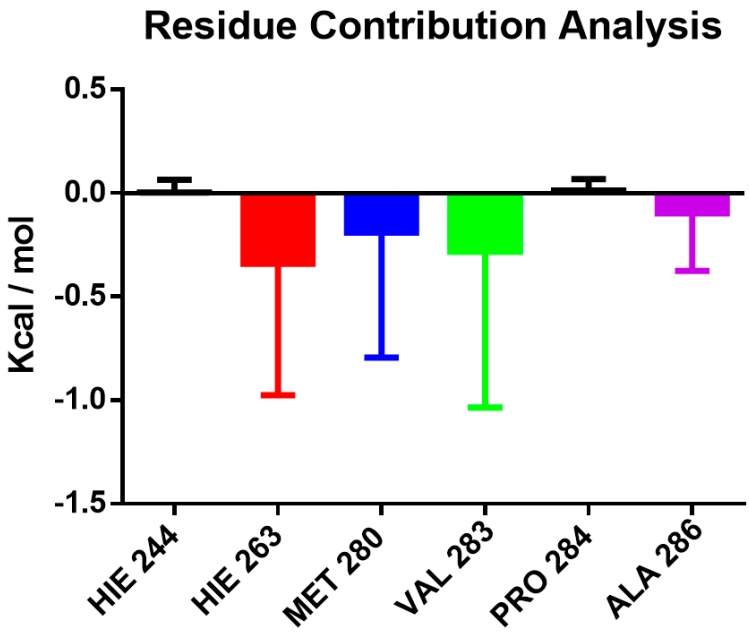

(b)

Preprints (www.preprints.org) | NOT PEER-REVIEWED | Posted: 14 November 2018 doi:10.20944/preprints201811.0330.v1

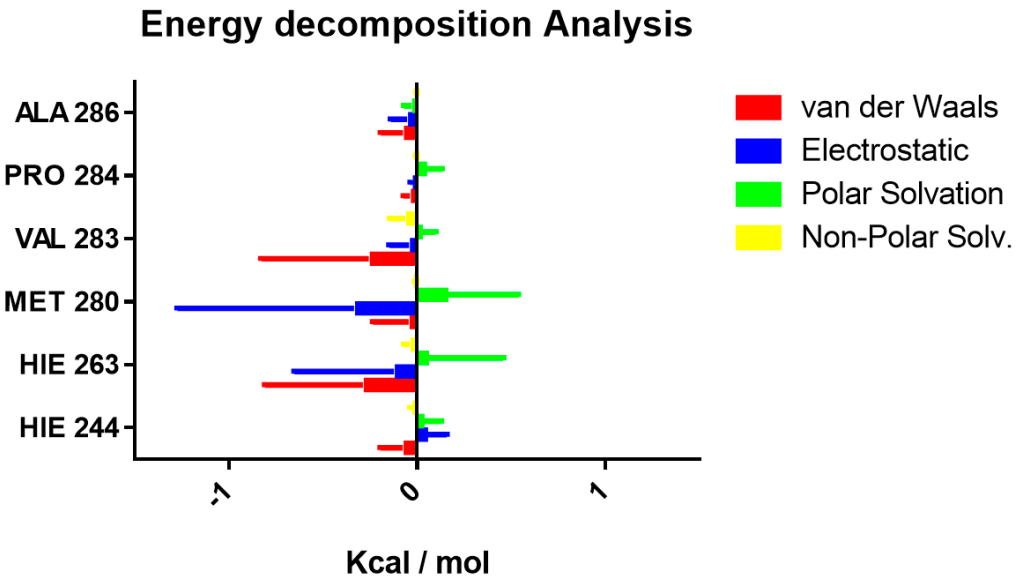

174

175 (c)

176 **Figure 3**. MD Results of compound 3g and tyrosinase. (a): Binding energy difference of complex
177 3g-tyrosinase, (delta total: total binding free energy; DELTA G solv: total solvation free energy;
178 DELTA G gas: Total gas phase free energy; ESURF: Non-polar solvation energy; EGB: Polar
179 solvation energy; EEL: Electrostatic energy; VDWAALS: van der Waals energy). (b): Residue
180 contributions of potential hot residues (potential hot residues are decorated in different colors
181 meanwhile not-potential hot residues are decorated in black). (c): Energy decomposition of
182 potential hot residues. For all energies, unit is Kcal/mol.

183

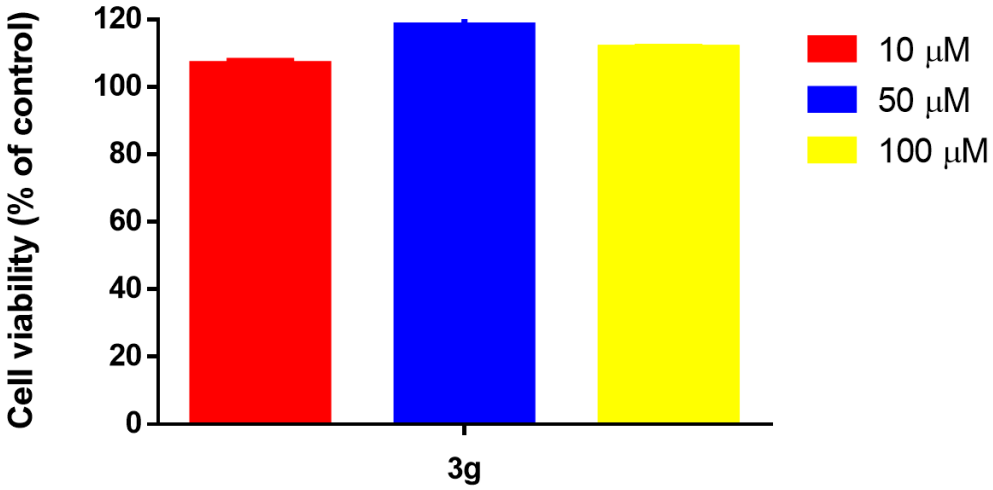

184

185 **Figure 4**. Effect of compound 3g on cell viability. Cells were treated with various concentrations of
186 compound 3g (10-100 μM), and examined by using CCK-8 assay. Values represents the mean ± SE
187 of three experiments. Data are expressed as % cell viability.

Preprints (www.preprints.org) | NOT PEER-REVIEWED | Posted: 14 November 2018 doi:10.20944/preprints201811.0330.v1

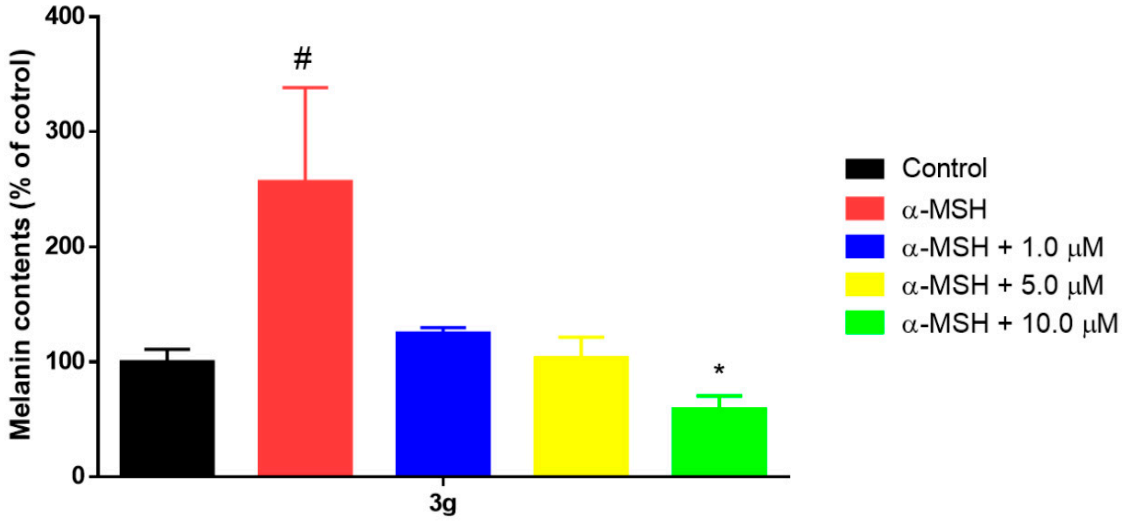

Figure 5. Ability of compound 3g to inhibit melanogenesis after treatment with 100 nM α-MSH in B16-F10 melanoma cells. Melanin levels were measured at 405 nm. Data are expressed as percentages of the control, and the values are expressed as the mean ± SE of three determinations. #$p < 0.05$ vs. the untreated control group; *$p < 0.05$ vs. the group treated with 100 nM α-MSH alone.

We then explored whether compound 3g that showed good tyrosinase inhibition activity was cytotoxic to B16-F10 melanoma cells. The CCK-8 assay was used to estimate the cytotoxicity of 3g and the results indicated that compound 3g was not cytotoxic up to 100 μM (Figure 4). Next, we quantified the melanin content in B16-F10 melanoma cells treated with 3g to assess its inhibitory effects on melanogenesis. As shown in Figure 5, compound 3g could effectively decreased melanin production stimulated by the α-MSH in a dose-related manner. The percentage of cellular melanin content following treatment with compound 3g was 125.07% at 1 μM, 103.75% at 5 μM, and 59.08% at 10 μM, compared to 100 nM α-MSH alone (256.72%) and the control group without using α-MSH (100%). Based on cytotoxic results, the inhibition of melanogenesis by compound 3g did not appear to be due to either cytotoxic effects or cell growth inhibition. The suppression of melanogenesis by compound 3g could be attributed to its inhibition of murine-derived tyrosinase[13].

3. Materials and Methods

3.1. General

Mushroom tyrosinase (T3824), L-tyrosine (91515), L-DOPA (D9628) were purchased from Sigma-Aldrich (Shanghai, China). α-MSH (ab120189) was purchased from Abcam (Shanghai, China). Synthetic melanin (M8631) and other chemical reagents were purchased from Aldrich (Shanghai, China). Murine B16-F10 melanoma cells were obtained from Shanghai Institutes for Biological Sciences, Chinese Academy of Sciences.

1H and 13C NMR spectra were measured on a Bruker Advance AC-300 spectrometer. MS spectra were recorded on a Mariner Mass Spectrum (ESI) or a LC/MSD TOF HR-MS Spectrum. Melting points were determined on Mel-TEMP II melting point apparatus. Shimadzu 160 spectrophotometer was used in the biological assays.

 doi:10.20944/preprints201811.0330.v1

3.2. Chemical Synthesis

3.2.1 General Procedure for the Preparation of Compounds (3a - 3l):

To a solution of 1 (3 g, 30 mmol) in toluene (70 mL) was added acrylic acid (2 g, 30 mmol) and Amberlyst 15 (5 g), and the mixture was stirred and refluxed for 2 h. The mixture was then filtered to remove Amberlyst 15, and the filtrate was removed under vacuum and subjected to silica-gel column chromatography (PE : EA = 4 : 1) to give the 2 as white powder. To a solution of 2 (0.4 g, 2.44 mmol) in DMF (2 mL) was added the specific amine (3 eq). The mixture was stirred for 12 h at 100 °C. Upon completion (TLC), H2O and EA were added and the layers separated. The organic layer was washed with brine, dried over anhydrous Na2SO4, concentrated under reduced pressure and then subjected to silica-gel column chromatography (CH2Cl2 : MeOH = 30 : 1) to give the target product.

7-Hydroxychroman-2-one (2)

White powder; Yield 45%; Mp = 162-163 °C (Previous literature reported mp = 162-163 °C).

3-(2,4-Dihydroxyphenyl)-1-(pyrrolidin-1-yl)propan-1-one (3a)

White powder; Yield 85%; Mp = 137-139 °C; 1H NMR (300 MHz, CDCl3，δ ppm): 8.21 (s, 1H), 7.98 (s, 1H), 6.84 (d, J = 8.2 Hz, 1H), 6.43 (d, J = 2.5 Hz, 1H), 6.35 (dd, J = 8.2, 2.5 Hz, 1H), 3.47 (s, 2H), 3.41 (t, J = 6.7 Hz, 4H), 3.29 (d, J = 6.8 Hz, 2H), 2.83 - 2.79 (m, 2H), 2.59 - 2.55 (m, 2H); 13C NMR (151 MHz, DMSO, δ ppm): 171.5 (C), 156.9 (C), 156.2 (C), 130.7 (CH), 118.4 (C), 106.4 (CH), 102.9 (CH), 41.7 (CH2), 33.5 (CH2), 25.9 (CH2), 14.6 (CH2), 13.5 (CH2); HRMS (ESI) m/z calcd for C13H17NO3 [M + H]+ 236.1281; found 236.1276.

3-(2,4-Dihydroxyphenyl)-1-(piperidin-1-yl)propan-1-one (3b)

Yellow powder; Yield 80%; Mp = 102-105 °C; 1H NMR (300 MHz, DMSO-d6, δ ppm): 9.24 (br s, 1H, -OH), 8.97 (br s, 1H, -OH), 6.81 (d, J = 8.2 Hz, 1H), 6.24 (d, J = 1.8 Hz, 1H), 6.13 (dd, J = 8.2 Hz, 1.8Hz, 1H), 3.40 (m, 2H), 3.28 (m, 2H), 2.57 (d, J = 6.1 Hz, 2H), 2.45 (d, J = 6.1 Hz, 2H), 1.57 (m, 2H), 1.35-1.44 (m, 4H); 13C NMR (151 MHz, DMSO, δ ppm): 171.0 (C), 156.9 (C), 156.2 (C), 130.7 (CH), 118.5 (C), 106.4 (CH), 103.0 (CH), 46.3 (CH2), 45.7 (CH2), 35.3 (CH2), 26.0 (CH2), 25.1 (CH2), 24.4 (CH2); HRMS (ESI) m/z calcd for C14H19NO3 [M + H]+ 250.1438; found 250.1447.

3-(2,4-Dihydroxyphenyl)-1-morpholinopropan-1-one (3c)

Yellow powder; Yield 87%; Mp = 155-157 °C; 1H NMR (300 MHz, DMSO-d6, δ ppm): 9.15 (br s, 1H, -OH), 9.89 (br s, 1H, -OH), 6.73 (d, J = 8.2 Hz, 1H), 6.16 (d, J = 1.8 Hz, 1H), 6.03 (dd, J = 8.2 Hz, 1.8Hz, 1H), 3.41 (m, 4H), 3.36 (m, 4H), 2.51 (d, J = 6.1 Hz, 2H), 2.38 (m, 2H); 13C NMR (151 MHz, DMSO, δ ppm): 171.3 (C), 157.0 (C), 156.2 (C), 130.7 (CH), 118.1 (C), 106.4 (CH), 102.8 (CH), 66.5 (CH2), 66.5 (CH2), 45.8 (CH2), 41.8 (CH2), 33.4 (CH2), 25.8 (CH2); HRMS (ESI): m/z calcd for C13H17NO4 [M + H]+: 252.1230, found: 252.1231.

N-(tert-butyl)-3-(2,4-dihydroxyphenyl)propanamide (3d)

White powder; Yield 86%; Mp = 142-144 °C; 1H NMR (300 MHz, DMSO-d6, δ ppm)：δ 9.11 (s, 1H), 8.92 (s, 1H), 7.32 (s, 1H), 6.79 (d, J = 8.2 Hz, 1H), 6.25 (d, J = 2.4 Hz, 1H), 6.11 (dd, J = 8.1, 2.4 Hz, 1H), 2.58 (m, J = 8.9, 6.6 Hz, 2H), 2.21 (m, J = 8.9, 6.7 Hz, 2H), 1.23 (s, 9H); 13C NMR (151 MHz, DMSO, δ ppm): 172.1 (C), 156.7 (C), 156.1 (C), 130.3 (CH), 118.5 (C), 106.3 (CH), 102.8 (CH), 50.2 (C), 36.2 (CH2), 29.0 (CH3), 25.5 (CH2); HRMS (ESI): m/z calcd for C13H19NO3 [M + H]+: 238.1438, found: 238.1431.

3-(2,4-Dihydroxyphenyl)-N,N-diethylpropanamide (3e)

White powder; Yield 90%; Mp = 132-133 °C; 1H NMR (300 MHz, DMSO-d6, δ ppm): 9.21 (br s, 1H, -OH), 8.95 (br s, 1H, -OH), 6.79 (d, J = 8.2 Hz, 1H), 6.23 (d, J = 1.8 Hz, 1H), 6.09 (dd, J = 8.2 Hz, 1.8Hz, 1H), 3.24 (m, 2H), 3.22 (m, 2H), 2.59 (d, J = 6.1 Hz, 2H), 2.41 (d, J = 6.1 Hz, 2H), 1.03 (t, J = 6.1 Hz, 3H), 0.97 (t, J = 6.1 Hz, 3H); 13C NMR (151 MHz, DMSO, δ ppm): 172.2 (C), 156.7 (C), 156.1 (C),

 doi:10.20944/preprints201811.0330.v1

130.3 (CH), 118.5 (C), 106.3 (CH), 102.8 (CH), 50.2 (CH2), 37.0 (CH2), 29.0 (CH2), 25.5 (CH3); HRMS (ESI): m/z calcd for C13H19NO3 [M + H]+: 238.1438, found: 238.1432.

3-(2,4-Dihydroxyphenyl)-N,N-dipropylpropanamide (3f)

White powder; Yield 85%; Mp = 129-130 °C; 1H NMR (300 MHz, CDCl3, δ ppm): 6.85 (d, J = 8.2 Hz, 1H), 6.46 (s, 1H), 6.38 (d, J = 8.2 Hz, 1H), 3.24 (m, 2H), 3.13 (m, 2H), 2.84 (d, J = 6.1 Hz, 2H), 2.64 (d, J = 6.1 Hz, 2H), 1.46-1.53 (m, 4H), 0.79-0.88 (m, 6H, -CH3*2); 13C NMR (151 MHz, DMSO, δ ppm): 172.7 (C), 157.0 (C), 156.3 (C), 130.6 (CH), 118.3 (C), 106.4 (CH), 102.9 (CH), 54.9 (CH2), 52.8 (CH2), 33.9 (CH2), 27.8 (CH2), 26.5 (CH2), 26.4 (CH2), 20.5 (CH3), 20.2 (CH3); HRMS (ESI): m/z calcd for C15H23NO3 [M + H]+: 266.1751, found: 266.1761.

N,N-dibutyl-3-(2,4-dihydroxyphenyl)propanamide (3g)

Light yellow oil; Yield 82%; 1H NMR (300 MHz, CDCl3, δ ppm): 6.86 (d, J = 8.2 Hz, 1H), 6.45 (s, 1H), 6.37 (d, J = 8.2 Hz, 1H), 3.28 (m, 2H), 3.16 (m, 2H), 2.85 (d, J = 6.1 Hz, 2H), 2.64 (d, J = 6.1 Hz, 2H), 1.40-1.48 (m, 4H), 1.20-1.30 (m, 4H), 0.86-0.93 (m, 6H, -CH3*2); 13C NMR (151 MHz, DMSO, δ ppm): 171.9 (C), 157.0 (C), 156.3 (C), 130.7 (CH), 118.3 (C), 106.4 (CH), 102.9 (CH), 47.3 (CH2), 45.2 (CH2), 33.6 (CH2), 31.2 (CH2), 30.0 (CH2), 26.2 (CH2), 20.1 (CH2), 19.9 (CH2), 14.2 (CH3), 14.1 (CH3); HRMS (ESI): m/z calcd for C17H27NO3 [M + H]+: 294.2064, found: 294.2070.

3-(2,4-Dihydroxyphenyl)-N,N-diisobutylpropanamide (3h)

Yellow oil; Yield 82%; 1H NMR (300 MHz, CDCl3, δ ppm): 9.55 (s, 1H), 6.88 (d, J = 8.2 Hz, 1H), 6.44 (d, J = 2.5 Hz, 1H), 6.36 (dd, J = 8.2, 2.5 Hz, 1H), 6.21 (s, 1H), 3.20 (d, J = 7.6 Hz, 2H), 3.06 (d, J = 7.6 Hz, 2H), 2.86 (m, 2H), 2.71 (m, 2H), 2.00 - 1.87 (m, 2H), 0.84 (dd, J = 13.8, 6.7 Hz, 12H); 13C NMR (75 MHz, DMSO, δ ppm): 172.8 (C), 157.0 (C), 156.3 (C), 130.6 (CH), 118.3 (C), 106.4 (CH), 103.3 (CH), 55.0 (CH2), 52.8 (CH2), 33.9 (CH2), 27.8 (CH2), 26.5 (CH2), 26.3 (CH2), 20.4 (CH3), 20.19 (CH3); HRMS (ESI): m/z calcd for C17H27NO3 [M + H]+: 294.2064, found: 294.2073.

3-(2,4-Dihydroxyphenyl)-N-(p-tolyl)propanamide (3i)

White powder; Yield 85%; Mp = 130-132 °C; 1H NMR (300 MHz, DMSO, δ ppm): 9.75 (s, 1H), 9.17 (s, 1H), 8.97 (s, 1H), 7.46 (d, J = 7.7 Hz, 2H), 7.08 (d, J = 8.0 Hz, 2H), 6.83 (d, J = 8.2 Hz, 1H), 6.27 (s, 1H), 6.12 (d, J = 8.2 Hz, 1H), 2.69 (m, J = 7.4 Hz, 2H), 2.47 (m, J = 7.3 Hz, 2H), 2.24 (s, 3H); 13C NMR (151 MHz, CDCl3, δ ppm): 174.1 (C), 157.9 (C), 156.5 (C), 156.4 (C), 155.5 (C), 131.3 (CH), 130.8 (CH), 129.5 (CH), 120.70 (CH), 107.6 (CH), 107.4 (CH), 104.8 (CH), 35.5 (CH2), 23.9 (CH2), 20.8 (CH3); HRMS (ESI): m/z calcd for C16H17NO3 [M + H]+: 272.1281, found: 272.1288.

3-(2,4-Dihydroxyphenyl)-N-(4-isopropylphenyl) propanamide (3j)

White powder; Yield 86%; Mp 142-145 °C; 1H NMR (300 MHz, DMSO, δ ppm): 9.76 (s, 1H), 9.17 (s, 1H), 8.97 (s, 1H), 7.48 (d, J = 8.1 Hz, 2H), 7.14 (d, J = 8.1 Hz, 2H), 6.83 (d, J = 8.1 Hz, 1H), 6.27 (s, 1H), 6.12 (d, J = 7.9 Hz, 1H), 2.81 (m, J = 4.9 Hz, 1H), 2.71 (m, J = 7.7 Hz, 2H), 2.47 (m, J = 7.5 Hz, 2H), 1.17 (d, J = 6.7 Hz, 6H); 13C NMR (151 MHz, DMSO, δ ppm): 171.2 (C), 156.9 (C), 156.2 (C), 143.4 (C), 137.5 (C), 130.4 (CH), 126.7 (CH), 119.6 (C), 118.1 (CH), 106.3 (CH), 102.8 (CH), 37.2 (CH2), 33.3 (CH), 25.5 (CH2), 24.4 (CH3); HRMS (ESI): m/z calcd for C18H21NO3 [M + H]+: 300.1594, found: 300.1598.

3-(2,4-Dihydroxyphenyl)-N-(4-methoxyphenyl) propanamide (3k)

White powder; Yield 90%; Mp 149-152 °C; 1H NMR (300 MHz, DMSO, δ ppm): 9.70 (s, 1H), 9.17 (s, 1H), 8.98 (s, 1H), 7.49 (d, J = 8.7 Hz, 2H), 6.85 (t, J = 7.7 Hz, 3H), 6.27 (s, 1H), 6.12 (d, J = 8.2 Hz, 1H), 3.71 (s, 3H), 2.69 (m, J = 7.8 Hz, 2H), 2.47 (m, 2H); 13C NMR (151 MHz, DMSO, δ ppm): 171.0 (C), 156.9 (C), 156.2 (C), 155.4 (C), 132.9 (C), 130.4 (CH), 121.0 (CH), 118.2 (CH), 114.2 (CH), 106.3 (CH), 102.8 (CH), 55.5 (CH3), 37.2 (CH2), 25.6 (CH2); HRMS (ESI): m/z calcd for C16H17NO4 [M + H]+: 288.1230, found: 288.1236.

 doi:10.20944/preprints201811.0330.v1

3-(2,4-Dihydroxyphenyl)-N-phenylpropanamide (3l)

White powder; Yield 92%; Mp 150-152 °C; 1H NMR (300 MHz, DMSO, δ ppm): 9.86 (s, 1H), 9.25 (s, 1H), 9.05 (s, 1H), 7.57 (d, J = 8.1 Hz, 2H), 7.28 (t, J = 7.6 Hz, 2H), 7.01 (t, J = 7.4 Hz, 1H), 6.84 (d, J = 7.9 Hz, 1H), 6.26 (s, 1H), 6.12 (d, J = 8.0 Hz, 1H), 2.70 (d, J = 7.7 Hz, 2H), 2.50 (s, 2H); 13C NMR (151 MHz, DMSO, δ ppm): 171.5 (C), 156.9 (C), 156.2 (C), 139.8 (C), 130.4 (CH), 129.1 (CH), 123.3 (CH), 119.5 (CH), 118.1 (CH), 106.3 (CH), 102.8 (CH), 37.3 (CH2), 25.5 (CH2); HRMS (ESI): m/z calcd for C15H15NO3 [M + H]+: 258.1125, found: 258.1128.

3.2.2 General Procedure for the Preparation of Compounds (5a - 5f, 7):

A solution of phenylpropionic acid (0.2g) in CH2Cl2 (10 mL) was stirred at room temperature for 60 min. Then CDI (1.2 eq) was added and stirred at room temperature for another 12 h. Upon completion (TLC), H2O were added and the layers separated. The organic layer was washed with brine, dried over anhydrous Na2SO4, concentrated under reduced pressure and then subjected to silica-gel column chromatography (CH2Cl2 : MeOH = 30 : 1) to give the product as light yellow oil.

N,N-dibutyl-3-(2,4-dimethoxyphenyl)propanamide (5a)

Light yellow oil; Yield 91%; 1H NMR (300 MHz, CDCl3, δ ppm): 7.09 (d, J = 8.1 Hz, 1H), 6.48 - 6.38 (m, 2H), 3.81 (d, J = 2.8 Hz, 6H,-OCH3*2), 3.37 - 3.25 (m, 2H), 3.24 - 3.10 (m, 2H), 2.94 - 2.80 (m, 2H), 2.62 - 2.46 (m, 2H), 1.58 - 1.42 (m, 4H), 1.29 (m, J = 5.8 Hz, 5H), 0.93 (m, J = 7.2 Hz, 6H,-CH3*2); 13C NMR (151 MHz, CDCl3, δ ppm): 172.4 (C), 159.4 (C), 158.3 (C), 130.5 (CH), 122.0 (C), 103.7 (CH), 98.4 (CH), 55.3 (CH3), 55.1 (CH3), 47.6 (CH2), 45.6 (CH2), 33.6 (CH2), 31.2 (CH2), 29.9 (CH2), 26.5 (CH2), 20.29, 20.11, 13.9 (CH3), 13.8 (CH3); HRMS (ESI): m/z calcd for C19H31NO3 [M + H]+: 322.2377, found: 322.2385.

N,N-dibutyl-3-(2-hydroxyphenyl)propanamide (5b)

Light yellow oil; Yield 84%; 1H NMR (300 MHz, CDCl3,,δ ppm): 9.78 (s, 1H), 7.18 - 7.04 (m, 2H), 6.93 (d, J = 8.0 Hz, 1H), 6.84 (t, J = 7.3 Hz, 1H), 3.40 - 3.26 (m, 2H), 3.25 - 3.13 (m, 2H), 3.02 - 2.86 (m, 2H), 2.80 - 2.67 (m, 2H), 1.57 - 1.42 (m, 4H), 1.36 - 1.20 (m, 4H), 0.93 (m, J = 13.0, 7.0 Hz, 6H, -CH3*2); 13C NMR (151 MHz, CDCl3, δ ppm): 173.4 (C), 155.5 (C), 130.6 (CH), 128.3 (C), 127.9 (CH), 119.9 (CH), 117.9 (CH), 47.7 (CH2), 46.4 (CH2), 34.9 (CH2), 30.6 (CH2), 29.6 (CH2), 24.9 (CH2), 20.2 (CH2), 20.1 (CH2), 13.8 (CH3), 13.8 (CH3); HRMS (ESI): m/z calcd for C18H29NO2 [M + H]+: 292.2271, found: 292.2266.

N,N-dibutyl-3-(4-hydroxyphenyl)propanamide (5c)

Light yellow oil; Yield 92%; 1H NMR (300 MHz, CDCl3, δ ppm): 9.78 (s, 1H), 7.14 (d, J = 7.8 Hz, 1H), 7.07 (d, J = 7.5 Hz, 1H), 6.93 (d, J = 8.0 Hz, 1H), 6.84 (t, J = 7.3 Hz, 1H), 3.37 - 3.27 (m, 2H), 3.23 - 3.15 (m, 2H), 3.02 - 2.93 (m, 2H), 2.78 - 2.69 (m, 2H), 1.56 - 1.42 (m, 4H), 1.36 - 1.19 (m, 4H), 0.93 (m, J = 13.0, 7.0 Hz, 6H, -CH3*2); 13C NMR (151 MHz, CDCl3, δ ppm): 172.5 (C), 154.9 (C), 129.4 (C), 129.1 (CH), 121.8 (CH), 115.4 (CH), 47.9 (CH2), 46.0 (CH2), 35.4 (CH2), 31.1 (CH2), 30.1 (CH2), 29.8 (CH2), 20.2 (CH2), 20.0 (CH2), 20.0 (CH2), 13.8 (CH3), 13.8 (CH3); HRMS (ESI): m/z calcd for C18H29NO2 [M + H]+: 292.2271, found: 292.2265.

N,N-dibutyl-3-(3,4-dihydroxyphenyl)propanamide (5d)

Light yellow oil; Yield 86%; 1H NMR (300 MHz, CDCl3, δ ppm): 6.94 (d, J = 7.9 Hz, 1H), 6.87 (d, J = 6.1 Hz, 1H), 6.73 (d, J = 6.7 Hz, 1H), 3.40 (m, J = 13.2, 5.8 Hz, 2H), 3.38 - 3.30 (m, 2H), 2.89 (m, J = 7.5 Hz, 2H), 2.63 (m, J = 14.5, 7.4 Hz, 2H), 1.75 - 1.54 (m, 4H), 1.48 - 1.25 (m, 4H), 0.97 (d, J = 7.4 Hz, 6H,-CH3*2); 13C NMR (151 MHz, CDCl3, δ ppm): 178.0 (C), 155.3 (C), 147.9 (C), 139.0 (C), 138.5 (CH), 122.1 (CH), 118.7 (CH), 47.9 (CH2), 47.6 (CH2), 35.7 (CH2), 35.6 (CH2), 30.7 (CH2), 30.1 (CH2), 30.0 (CH2), 20.0 (CH2), 20.0 (CH2), 13.8 (CH3); HRMS (ESI): m/z calcd for C17H27NO3 [M + H]+: 294.2064, found: 294.2069.

N,N-dibutyl-3-(2-chlorophenyl)propanamide (5e)

Light yellow oil; Yield 89%; 1H NMR (300 MHz, DMSO, δ ppm): 7.41 (d, J = 7.6 Hz, 1H), 7.35 (d, J = 6.7 Hz, 1H), 7.30 - 7.19 (m, 2H), 3.26 - 3.13 (m, 4H), 2.92 (m, J = 7.7 Hz, 2H), 2.56 (m, J = 7.7 Hz, 2H), 1.40 (m, 4H), 1.21 (m, J = 7.1 Hz, 4H), 0.86 (m, J = 7.1 Hz, 6H, -CH3*2); 13C NMR (151 MHz, CDCl3, δ ppm): 178.1 (C), 137.8 (C), 133.9 (C), 130.4 (CH), 129.6 (CH), 127.9 (CH), 126.9 (CH), 47.9 (CH2), 46.0 (CH2), 32.9 (CH2), 31.1 (CH2), 30.0 (CH2), 28.7 (CH2), 20.2 (CH2), 20.0 (CH2), 13.9 (CH3), 13.8 (CH3); HRMS (ESI): m/z calcd for C17H26ClNO [M + H]+: 296.1776, found: 296.1773.

N,N-dibutyl-3-(4-chlorophenyl)propanamide (5f)

Light yellow oil; Yield 83%; 1H NMR (300 MHz, CDCl3, δ ppm): 7.25 (d, J = 8.2 Hz, 2H), 7.16 (d, J = 8.2 Hz, 2H), 3.36 - 3.25 (m, 2H), 3.19 - 3.08 (m, 2H), 2.96 (t, J = 7.7 Hz, 2H), 2.57 (t, J = 7.7 Hz, 2H), 1.55 - 1.40 (m, 4H), 1.36 - 1.21 (m, 4H), 0.92 (m, J = 8.1, 6.3 Hz, 6H, -CH3*2); 13C NMR (151 MHz, CDCl3, δ ppm): 171.2 (C), 140.1 (C), 131.7 (C), 129.8 (CH), 128.5 (CH), 47.7 (CH2), 45.8 (CH2), 34.8 (CH2), 31.1 (CH2), 30.9 (CH2), 29.9 (CH2), 20.2 (CH2), 20.1 (CH2), 13.9 (CH3), 13.8 (CH3); HRMS (ESI): m/z calcd for C17H26ClNO [M + H]+: 296.1776, found: 296.1767.

N,N-dibutyl-3-(4-chlorophenoxy)propanamide (7)

Light yellow oil; Yield 91%; 1H NMR (300 MHz, CDCl3, δ ppm): 7.23 (d, J = 8.8 Hz, 2H), 6.85 (d, J = 8.6 Hz, 2H), 4.31 (t, J = 6.7 Hz, 2H), 3.50 - 3.17 (m, 4H), 2.82 (t, J = 6.7 Hz, 2H), 1.73 - 1.46 (m, 4H), 1.34 (dt, J = 15.5, 7.7 Hz, 4H), 1.07 - 0.81 (m, 6H, -CH3*2); 13C NMR (151 MHz, CDCl3, δ ppm): 169.4 (C), 154.6 (C), 129.4 (C), 125.1 (CH), 116.7 (CH), 52.7 (CH2), 50.2 (CH2), 30.7 (CH2), 29.7 (CH2), 29.6 (CH2), 20.1 (CH2), 19.8 (CH2), 13.8 (CH3), 13.4 (CH3); HRMS (ESI): m/z calcd for C17H26ClNO2 [M + H]+: 311.1652, found: 311.1662.

3.3. In Vitro Tyrosinase Inhibition Assay

The inhibition of target compounds on the monophenolase and diphenolase activity of mushroom tyrosinase were carried out according to the method reported by Wei Yi et al [14] with some modifications，using L-tyrosine or L-DOPA as substrate, respectively. All the inhibitors were dissolved in methanol and phosphate buffer (pH = 6.8) was utilized to dilute the methanol stock solution of test compounds. The test samples were first pre-incubated with L-tyrosine or L-DOPA solution (1.25 mM), in 0.05 M phosphate buffer solution (pH 6.8), for 10 min at 25 °C. Then, 5 μL of mushroom tyrosinase solution (333 U/mL) was added to the mixture. The assay mixture containing L-tyrosine was incubated at 25 °C for 30 min, and the assay mixture containing L-DOPA was incubated at 25 °C for 5 min. The amount of DOPAchrome produced in the reaction mixture was determined at 475 nm in the microplate reader. The percentage of the inhibition of mushroom tyrosinase activity was calculated as following: inhibition (%) = [(A - B) - (C - D)]/(A – B) x 100, where A is the absorbance of assay buffer and enzyme, B is the absorbance of assay buffer, C is the absorbance of assay buffer, test sample and enzyme, D is the absorbance of assay buffer and test sample. All experiments were performed in triplicate. Calculation of the IC50 values was performed with Graph Pad Prism 5.0. As the positive control, the IC50 of kojic acid was also determined.

3.4. In Vitro Cytotoxicity Assay

Cell viability was measured by the WST-8 [2-(2-methoxy-4-nitrophenyl)-3-(4-nitrophenyl)-5-(2,4-disulfophenyl)-2H-tetrazolium, monosodium salt] assay using CCK-8. Briefly, 100 μL of B16-F10 melanoma cell suspension was dispensed in a 96-well plate (5,000 cells/well). After 24 h incubation of cells in a humidified incubator, various concentrations of test compounds were added into the culture media in the plate (25 μL/well). The plate was incubated at 37 °C in a humidified incubator with 5% (v/v) CO2 for 48 h. After removing original culture medium, fresh complete medium containing CCK-8 solution (10 %) was added to each well of the plate, and the reaction mixture was further incubated for 1h at 37 °C. The absorbance at 450 nm was measured using a microplate reader with a reference filter of 650 nm. The percentage of cell growth inhibition was calculated by the following equation: growth inhibition (%) = [(A_c -

 doi:10.20944/preprints201811.0330.v1

$A_s)/(A_c - A_b)] \times 100$, where A_s is the absorbance from the cells incubated with CCK-8 and test compound, A_c is the absorbance from the cells incubated with CCK-8 and DMSO, and A_b is the background absorbance from medium containing CCK-8 and DMSO.

3.5. Melanin Biosynthesis Assay

The melanin assay was performed as previously reported[15]. B16-F10 cells were transferred to a 24-well plate at a density of 5 × 104 cells / well and incubated in the presence or absence of 100 nM α-MSH for 24 h. Cells were then treated with various concentrations of test compounds (0 - 10 μM) for a further 24 h. After removing culture medium, 100 μL of 1 N NaOH was added to each well. The samples were mixed immediately and incubated at 60 °C for 1 h to solubilize melanin. The amount of melanin in reaction mixture was determined according to spectrophotometric analysis at an absorbance of 405 nm. Absorbance at 405 nm was compared with a standard curve of synthetic melanin.

3.6. Molecular Docking

The structure of compound 3g was prepared in DS 3.0 and then minimized by 2000 steps of steepest decent method followed by 2000 steps of conjugate gradient method. The 3D structure of mushroom tyrosinase was downloaded from protein data bank (PDB ID: 2Y9X) and prepared by using the "Prepare protein" module in DS 3.0, with parameters set as default. The molecular docking simulation was performed by DS 3.0. The binding site is defined by residues around the native binder tropolone in radius 7.5 Å. Other parameters were kept as default. The intermolecular interactions were shown in DS 3.0.

3.7.Molecular dynamics (MD) simulations

MD simulations were performed using the PMEMD module in AMBER 16[16] accelerated by GPU system consist of the NVIDIA CUDA processor. The initial structures of 3g as the ligand docked with the receptor from PDB ID:2Y9X, the details have been described in the Molecular Docking section. The protein was assigned with the AMBER ff99SB force field[17], while the ANTECHAMBER module and the general AMBER force field (GAFF)[18] was applied to the ligand. All hydrogen atoms of the proteins and ligands were added using the reduce module. The systems were solvated in a TIP3P water box in a 9 Å hexahedron. Sodium ions were added with the purpose of neutralize the systems. To remove possible steric stresses, the systems were minimized for 1,0000 steps with the steepest descent method, followed by application of conjugate gradients for another 1,0000 steps. All two systems were linearly heated from 0 to 300 K using a Langevin thermostat and weak restraints of 10 kcal/mol on the protein backbone atoms over 1ns. Then the whole system was equilibrated in PMEMD with CPU code for 0.1ns to make the system density be converged. Finally, dynamics simulations of 100ns NPT ensemble at 1 atm and 300K. After MD simulation, 5000 frames were extracted from the 100 ns of trajectory for CPPTRAJ[19] analysis. The MMPBSA[20] method in the AMBER 16 was used to calculate the binding free energies and energy decomposition.

4. Conclusion

In conclusion, we obtained a highly potent tyrosinase inhibitor (3g) combining series synthesis ， in vitro enzyme inhibition assay and cellular activity assays. Structure-activity relationship study indicated that the 2,4-resorcinol moiety and terminal, minor bulky hydrophobic group were key pharmacophores required for potency of the novel 4-resorcinol derivatives, and modification of the ethylidene linker produced the analogue without any inhibitory potency. Moreover, we demonstrated that 3g could efficiently inhibit the melanin production in B16-F10 cells without affecting cell viability and proliferation. These results strongly indicated that compound 3g might be used as an new candidate for therapeutic agents in the treatment of diseases associated with hyperpigmentation.

Acknowledgments:

We gratefully thank the support from the Fundamental Research Funds for the Central Universities (XDJK2014C066，SWU113080).

Author Contributions:

X.Q. and Z.Y. conceived and designed the experiments; Z.Y., L.Q. and Y.H. performed the experiments; L.Q, F.R., Y.H. and C.Y. analyzed the data; M.J. and C.Y. contributed reagents/materials/analysis tools; Z.Y. and L.Q. wrote the paper.

Conflicts of Interest:

The authors declare no conflict of interest. The founding sponsors had no role in the design of the study; in the collection, analyses, or interpretation of data; in the writing of the manuscript, and in the decision to publish the results.

References

1. Bard, M.; Woods, R. A.; Barton, D. H.; Corrie, J. E.; Widdowson, D. A., Sterol mutants of Saccharomyces cerevisiae: chromatographic analyses. Lipids 1977, 12 (8), 645-54.
2. (a) Khan, K. M.; Maharvi, G. M.; Khan, M. T.; Jabbar Shaikh, A.; Perveen, S.; Begum, S.; Choudhary, M. I., Tetraketones: a new class of tyrosinase inhibitors. Bioorganic & medicinal chemistry 2006, 14 (2), 344-51; (b) Nerya, O.; Musa, R.; Khatib, S.; Tamir, S.; Vaya, J., Chalcones as potent tyrosinase inhibitors: the effect of hydroxyl positions and numbers. Phytochemistry 2004, 65 (10), 1389-1395.
3. Sugumaran, M., Molecular mechanisms for mammalian melanogenesis. Comparison with insect cuticular sclerotization. FEBS letters 1991, 295 (1-3), 233-9.
4. Okombi, S.; Rival, D.; Bonnet, S.; Mariotte, A. M.; Perrier, E.; Boumendjel, A., Discovery of benzylidenebenzofuran-3(2H)-one (aurones) as inhibitors of tyrosinase derived from human melanocytes. Journal of medicinal chemistry 2006, 49 (1), 329-33.
5. (a) Xu, Y.; Stokes, A. H.; Freeman, W. M.; Kumer, S. C.; Vogt, B. A.; Vrana, K. E., Tyrosine mRNA is expressed in human substantia nigra. Molecular Brain Research 1997, 45 (1), 159-162; (b) Asanuma, M.; Miyazaki, I.; Ogawa, N., Dopamine- or L-DOPA-induced neurotoxicity: the role of dopamine quinone formation and tyrosinase in a model of Parkinson's disease. Neurotox Res 2003, 5 (3), 165-76.
6. Fisk, W. A.; Agbai, O.; Levtov, H. A.; Sivamani, R. K., The use of botanically derived agents for hyperpigmentation: a systematic review. Journal of the American Academy of Dermatology 2014, 70 (2), 352-365.
7. Lee, S. Y.; Baek, N.; Nam, T. G., Natural, semisynthetic and synthetic tyrosinase inhibitors. Journal of enzyme inhibition and medicinal chemistry 2016, 31 (1), 1-13.
8. van Gelder, C. W.; Flurkey, W. H.; Wichers, H. J., Sequence and structural features of plant and fungal tyrosinases. Phytochemistry 1997, 45 (7), 1309-23.
9. Pillaiyar, T.; Namasivayam, V.; Manickam, M.; Jung, S. H., Inhibitors of Melanogenesis: An Updated Review. Journal of medicinal chemistry 2018, 61 (17), 7395-7418.
10. Mcevily, A. J., Inhibition of Polyphenol Oxidase by Phenolic Compounds. Acs Symposium 1992, 318-325.
11. Khatib, S.; Nerya, O.; Musa, R.; Tamir, S.; Peter, T.; Vaya, J., Enhanced substituted resorcinol hydrophobicity augments tyrosinase inhibition potency. Journal of medicinal chemistry 2007, 50 (11), 2676-81.
12. Gonzalez-Gomez, J. C.; Santana, L.; Uriarte, E., Regioselective Synthesis of Dihydrofuro[3,2-g]coumarin-6-one. 2003.
13. (a) Han, Y. K.; Park, Y. J.; Ha, Y. M.; Park, D.; Lee, J. Y.; Lee, N.; Yoon, J. H.; Moon, H. R.; Chung, H. Y., Characterization of a novel tyrosinase inhibitor, (2RS,4R)-2-(2,4-dihydroxyphenyl)thiazolidine-4-carboxylic

518 acid (MHY384). Biochimica et biophysica acta 2012, 1820 (4), 542-9; (b) Ha, Y. M.; Yun, J. P.; Ji, Y. L.; Park, D.;
519 Choi, Y. J.; Lee, E. K.; Ji, M. K.; Kim, J. A.; Ji, Y. P.; Lee, H. J., Design, synthesis and biological evaluation of
520 2-(substituted phenyl)thiazolidine-4-carboxylic acid derivatives as novel tyrosinase inhibitors. Biochimie 2012,
521 94 (2), 533-540.
522 14. You, A.; Zhou, J.; Song, S.; Zhu, G.; Song, H.; Yi, W., Structure-based modification of
523 3-/4-aminoacetophenones giving a profound change of activity on tyrosinase: from potent activators to highly
524 efficient inhibitors. European journal of medicinal chemistry 2015, 93, 255-62.
525 15. Bae, S. J.; Ha, Y. M.; Park, Y. J.; Park, J. Y.; Song, Y. M.; Ha, T. K.; Chun, P.; Moon, H. R.; Chung, H. Y.,
526 Design, synthesis, and evaluation of (E)-N-substituted benzylidene-aniline derivatives as tyrosinase inhibitors.
527 European journal of medicinal chemistry 2012, 57, 383-390.
528 16. Case, D. A.; Betz, R. M.; Cerutti, D. S.; Cheatham, T. E.; III; Darden, T. A.; Duke, R. E.; Giese, T. J.; Gohlke,
529 H.; Goetz, A. W., AMBER 2016, University of California, San Francisco. 2016.
530 17. Hornak, V.; Abel, R.; Okur, A.; Strockbine, B.; Roitberg, A.; Simmerling, C., Comparison of multiple amber
531 force fields and development of improved protein backbone parameters. Proteins 2006, 65 (3), 712-725.
532 18. Wei, Z.; Hou, T.; Xuebin Qiao, A.; Xu, X., Parameters for the Generalized Born Model Consistent with
533 RESP Atomic Partial Charge Assignment Protocol. J Phys Chem B 2003, 107 (34), 9071-9078.
534 19. Roe, D. R.; Cheatham, T. E., 3rd, PTRAJ and CPPTRAJ: Software for Processing and Analysis of Molecular
535 Dynamics Trajectory Data. J Chem Theory Comput 2013, 9 (7), 3084-95.
536 20. Iii, B. R. M.; Jr, M. G.; Swails, J. M.; Homeyer, N.; Gohlke, H.; Roitberg, A. E., MMPBSA.py: An Efficient
537 Program for End-State Free Energy Calculations. Journal of Chemical Theory & Computation 2012, 8 (9), 3314.

538

539 **Sample Availability:** Samples of the compounds are available from the authors.